Coexistence of LTE and WLAN in Unlicensed Bands: Full-Duplex Spectrum Sensing

Ville Syrjälä and Mikko Valkama
Department of Electronics and Communications Engineering
Tampere University of Technology
Tampere, Finland
ville.syrjala@tut.fi

Abstract—**Problem of opportunistic use of the unlicensed 5-GHz band for LTE carrier aggregation (LTE unlicensed) is studied from the point-of-view of cognitive full-duplex transceivers. In this paper, an initial study of the impact of self-interference on the performance of cyclostationary spectrum sensing algorithm is given, in case where a full-duplex transceiver tries opportunistically use parts of the band used by a WLAN signal. Effective sensing while transmitting is natively possible, because WLAN and LTE signals have different cyclic properties. The evaluation of the impact focuses on extensive system simulations and simulation analysis. It is concluded that the self-interference can indeed interfere with the cyclostationary spectrum sensing. However, the effect can be lowered by lowering the bandwidth of the aggregated signal and instead using higher spectral density for the lower bandwidth signal.**

Keywords—LTE unlicensed; full-duplex radio; spectrum sensing; cyclostationary spectrum sensing

I. INTRODUCTION

Ever-increasing growth in the use of mobile data requires that the available spectrum is used as efficiently as possible. Another solution to answer for the growth is to allocate more spectra for mobile data. One proposed solution to combine the both of these solutions is so called LTE-Unlicensed (LTE-U), in which Long Term Evolution (LTE) downlink is aggregated to the unlicensed 5-GHz band. Wireless LAN (WLAN) signals are already allocated to the unlicensed 5-GHz band, but aggregating LTE downlink is much simpler for LTE transceivers, than utilizing the WLAN simultaneously with licensed LTE for additional throughput. Furthermore, LTE provides higher spectral efficiency compared to WLAN, as well as longer range. However, the use of the unlicensed for carrier aggregation is more complicated than the use of licensed bands, because other systems already exist in the band. Therefore the coexistence methods need to be considered to enable LTE-U [1], [2].

One solution for the coexistence of aggregated LTE downlink and WLAN in the unlicensed bands is the cognitive radio technology based on opportunistic spectrum access [3], [4]. Unfortunately, even though opportunistic spectrum access has received huge amounts of research input in recent years, there have not been many practical implementations. This is natural, because the licensed users do not wish any additional interference to the bands allocated for them. In LTE-U, however, the idea is that open spectrum is used for carrier aggregation. This might still be fairly problematic, because the co-existence methods should be designed so that the existing systems are minimally interfered. To help this, this paper proposes use of wireless full-duplex technology to be used for opportunistic spectral access in LTE-U. This basically means that the opportunistic user (LTE user) can sense for the primary signal (WLAN), while it transmits the signals itself. This makes the whole opportunistic spectrum access more attractive, because the secondary user can react to the primary signal faster, since the sensing can be carried out all the time.

In the literature, it has been already shown that utilizing full-duplex technology for cognitive radio application offers many benefits over the traditional receiver architectures [5], [6], [7]. This paper carries out an initial study on what is the effect of the self-interference on the performance of cyclostationary spectrum sensing algorithm in LTE-U, and proposes the use of full-duplex radio technology for LTE-U. This enables listen-whilst-talking, instead of de facto listen-before-talk. This is promising, because WLAN and LTE signals have significantly different cyclic properties. This has not been considered in the existing literature. Special emphasis is given to study the effect of the bandwidth of the aggregated LTE signal on the performance of cyclostationary spectrum sensing. Specific coexistence strategies are not yet discussed in this paper.

The outline of this paper after this section is as follows. The second section shortly presents the general level ideas of full-duplex radio architecture and cyclostationary spectrum sensing, and shortly discusses the use of cognitive full-duplex radio technology in LTE-U. The third section then describes the simulator and simulation parameters, and the simulation results and the corresponding analysis are given in the fourth section. Finally, the fifth section concludes the work.
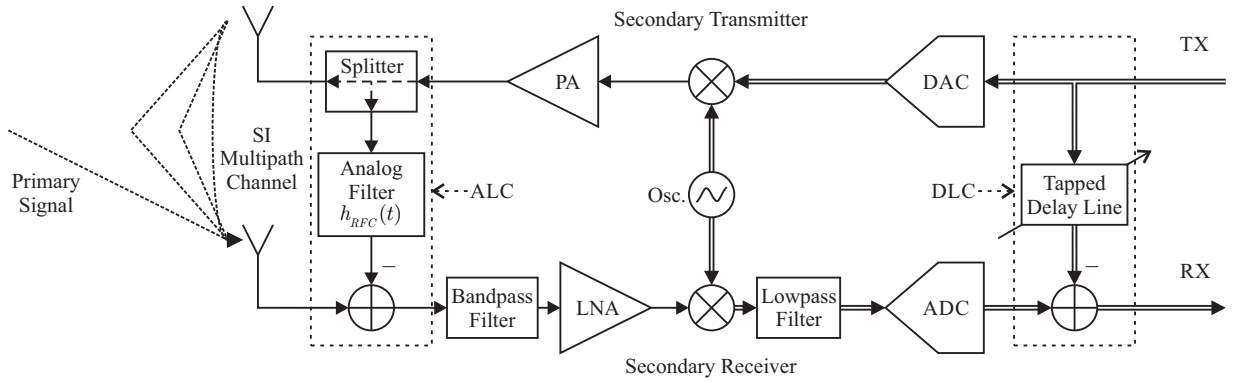
Fig. 1. Principal illustration of a cognitive full-duplex transceiver with analog linear cancellation (ALC) and digital linear cancellation (DLC) of the self interference.

II. COGNITIVE FULL-DUPLEX TRANSCEIVER UTLIZING CYCLOSTATIONARY SPECTRUM SENSING

This section shortly describes the cognitive full-duplex radio transceiver and the idea of using full-duplex cognitive radio transceivers combined with cyclostationary spectrum sensing.in LTE-U. Finally, cyclostationary spectrum sensing is presented in detail.

A. Cognitive Full-Duplex Radio Transceiver

Principal illustration of a cognitive full-duplex transceiver is given in Fig. 1. The basic principle is like in any modern direct conversion transceiver, but since the transmitter transmits at the same center frequency as the receiver receives, the own signal (called self-interference from now on) needs to be cancelled at the receiver. In the full-duplex transceiver structure of Fig. 1, this is done in two stages. First, an analog filter is tuned to match the self-interference channel as closely as possible in analog domain. Then, the signal to be transmitted is fed through the filter and subtracted from the received signal. The second stage of the cancellation is done in digital domain, where a digital filter mimics the remaining self-interference channel, and the cancellation is carried out using the transmitted samples. The digital cancellation is very important part even though the analog cancellation is done already in the analog domain, because of the limitations in analog-domain filtering. [8]

The cyclostationary spectrum sensing is done in the digital domain after both of the self-interference cancellation stages have been carried out.

B. Use of Full-Duplex Transceivers to Enable LTE-U

Usual solutions for coexistence in LTE-U are based on so-called listen-before-talk principle [1], [2]. The base station (secondary user) basically listens for the primary user and transmits if it does not exist, and then again stops transmission to listen. This is very inefficient, because of the pauses, but it also potentially causes interference to existing systems, if the primary system begins transmission right or shortly after the secondary user begins the transmission.

Using full-duplex radio technology in LTE-U offers two key benefits over the de facto listen-before-talk principle. With full-duplex radio technology so-called listen-whilst-talk principle can be utilized. First key benefit is that the LTE base station does not need to stop its transmission while sensing, because the sensing and transmission can be carried out simultaneously. The second key benefit is that when the sensing is done simultaneously with the transmission, the secondary user can react to the primary user transmission instantaneously and discontinue or change the transmission so that it does not interfere with the primary system.

The different cyclic properties of the LTE and WLAN signals enable the listen-whilst-talk principle. In LTE-U, cyclic frequencies of the primary and secondary signals are, very different. The primary signal is IEEE 802.11 family signal with 64 subcarriers and 8 or 16 sample cyclic prefix. The length of the OFDM symbol without cyclic prefix (cyclic delay) is 3.2 μs and with cyclic prefix 3.6 μs or 4 μs. The secondary signal on the other hand has totally different properties, e.g., the 10 MHz mode has 1024 subcarriers with 72 or 256 sample cyclic prefix. The length of the OFDM symbol without cyclic prefix (cyclic delay) is 66.67 μs and with cyclic prefix 71.35 μs or 83.33 μs. The cyclic frequencies, and more importantly, the cyclic delays are totally different. The timings of these signals and their relationship to the sensing period are illustrated in Fig. 2.

C. Cyclostationary Spectrum Sensing

The cyclostationary spectrum sensing algorithm used in this paper is based on the statistical tests proposed in [9]. For an OFDM signal $x(n)$, its conjugate cyclic autocorrelation function

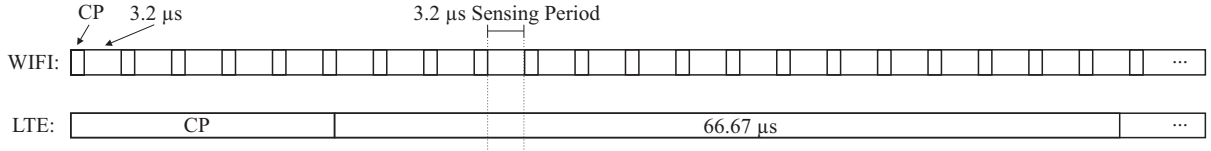$$R_x^{f_k} = \hat{R}_x^{f_k} + \varepsilon(f_k) \tag{1}$$

Fig. 2. An example illustration of different timings in WLAN signal with 16 sample cyclic prefix and LTE signal with 256 sample cyclic prefix. The signals are in correct relation to each others.

is non-zero for the cyclic frequencies of the OFDM signal $f_k \in A$ (A is a set of cyclic frequencies of the OFDM signal $x(n)$), and zero when $f_k \notin A$. In (1), $\varepsilon(f_k)$ is the estimation error in the sample estimate of the conjugate cyclic autocorrelation function

$$\hat{R}_x^{f_k} = \frac{1}{N} \sum_{n=0}^{N-1} x(n) x^*(n-\tau) e^{\frac{-j2\pi f_k n}{N}} . \tag{2}$$

Here, τ is the length of the OFDM signal with FFT length N without the cyclic prefix. The statistical test is based on the fact that the estimation error is asymptotically Gaussian distributed zero-mean complex random variable. The test can therefore be formulated for known cyclic frequencies $f_k \in A$ as a hypothesis test

$$\begin{aligned} H_0 &: \forall f_k \in A : \hat{R}_x^{f_k} = \varepsilon(f_k) \\ H_1 &: \exists f_k \in A : \hat{R}_x^{f_k} = R_x^{f_k} + \varepsilon(f_k) \end{aligned}, \tag{3}$$

where H_0 is a null hypothesis (the cyclostationary signal is not present) and H_1 is one-hypothesis (the cyclostationary signal exists). This is a very simple binary classification task, so the test can be formulated as a simple threshold test [9]. Notice that because of the motivation in the previous subsection, the residual self-interference is considered to be noise in this test, and therefore included in the estimation error.

Following the test proposed in [10], the threshold test for the presence of cyclostationarity, when the noise is assumed to be zero-mean Gaussian distributed, can be formulated into a simple form

$$F_{\chi^2}(T) > 1 - p, \tag{4}$$

where p is the desired false-alarm rate, F_{χ^2} denotes the cumulative distribution function of the well-known χ^2 distribution, and the χ^2 distributed test statistic can be computed as

$$T = \hat{R}_{x,v}^{f_k} \hat{\Sigma}_{2c}^{-1} (\hat{R}_{x,v}^{f_k})^T , \tag{5}$$

where vector

$$\hat{R}_{x,v}^{f_k} = \left[\operatorname{Re}\left\{ \hat{R}_x^{f_k} \right\} \quad \operatorname{Im}\left[\hat{R}_x^{f_k} \right] \right]. \tag{6}$$

In the computation of the test statistic T, the estimate of the covariance matrix of $\hat{R}_{x,v}^{f_k}$ can be written as

$$\hat{\Sigma}_{2c} = \begin{bmatrix} E\left[\operatorname{Re}\left\{ \hat{R}_x^{f_k} \right\}^2 \right] & E\left[\operatorname{Re}\left\{ \hat{R}_x^{f_k} \right\} \operatorname{Im}\left\{ \hat{R}_x^{f_k} \right\} \right] \\ E\left[\operatorname{Re}\left\{ \hat{R}_x^{f_k} \right\} \operatorname{Im}\left\{ \hat{R}_x^{f_k} \right\} \right] & E\left[\operatorname{Im}\left\{ \hat{R}_x^{f_k} \right\}^2 \right] \end{bmatrix}. \tag{7}$$

For computational simplicity this test assumes that the estimation error is zero-mean Gaussian distributed. In practice, this is not strictly the truth, because the residual self-interference contributes to the total noise of the system, and it only resembles a Gaussian distributed signal without strictly being one.

III. SIMULATOR

A. Simulation Routine

First, OFDM modulated signal waveforms are generated for the own transmitter (self-interference) and primary-user transmitter. The signals are not in any way synchronized to each other. Both signals are then put through independent multipath channels. Additive noise is generated and summed to the sum of the two signals. The total self-interference cancellation is modelled in two stages. First, the analog-domain self-interference cancellation is modelled, so that only the first multipath component of the self-interference signal is suppressed to the desired level. In this process, white Gaussian noise is used as an error to model the estimate of the first multipath component in the cancellation. Then, digital domain self-interference cancellation is modelled, which aims to cancel the other multipath components of the self-interference signal as well as to improve the cancellation of the first multipath component. Once again, white Gaussian noise is used as an estimation error in the digital self-interference cancellation algorithm. Therefore, the self-interference cancellation is not only modelled as a simple attenuation, but as a more realistic process.

The signal with self-interference partially cancelled is then fed to the cyclostationary spectrum sensing algorithm set to detect the primary user signal.

The simulator is using 20 MHz sampling rate. The primary-user signal is an OFDM signal with 312.5 kHz subcarrier spacing and with 64 subcarriers of which 52 around the center subcarrier are active and the remaining subcarriers are nulled. 16QAM subcarrier modulation is used, and cyclic prefix length is set to 8 samples per OFDM symbol. The self-interference signal (own signal) is an OFDM signal with 15 kHz subcarrier spacing and with 1024 subcarriers of which varying amount of subcarriers are active. The active subcarriers are always evenly around the center subcarrier and all the other subcarriers are nulled. 16QAM subcarrier modulation is also used for the self-interference signal. The signal is modelled by first generating the native LTE-signal samples with 15.36 MHz sampling rate. The signal is then 4-times oversampled, and then linear interpolation and filtering are then used to the signal samples, to get the samples from the correct positions to model the signal more accurately at the 20 MHz sampling rate. Linear interpolation gives rather accurate model since, the signal is relatively narrow-bandwidth compared to the sampling rate after the oversampling.

The cyclostationary spectrum sensing algorithm is set so that it gives 2 % false-alarm rate in the case that the only interferer is the white-Gaussian noise. The non-Gaussian statistical properties of the self-interference are the only reason for false-alarm rates that are not 2 % in the results, and without the self-interference the false-alarm rate is always on average 2 %.

IV. SIMULATION RESULTS AND ANALYSIS

In Fig. 3, the detection probability is given as a function of the primary-user signal-to-noise ratio. Different curves denote the different total power differences (in dB) between the self-
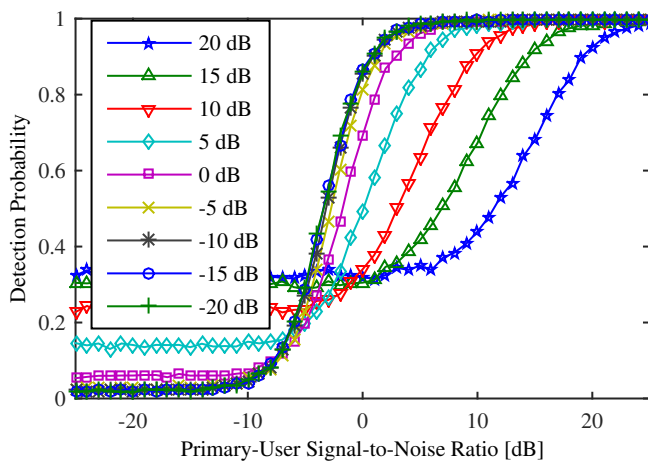

Fig. 3. Detection probability as a function of the primary-user signal-to-noise-ration when the total power of the self-interference after the self-interference cancellation stages is set the amount (in dB) denoted in the legend above the total additive white Gaussian noise power. The amount of active subcarriers (bandwidth) of the self-interference signal is 600 (full).
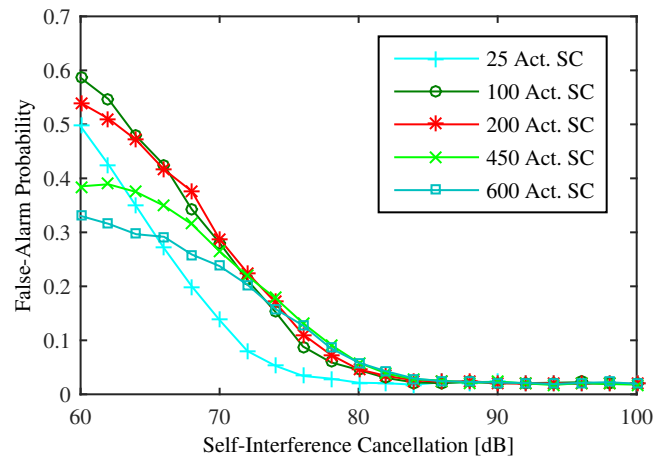

Fig. 4. False-alarm probability as a function of self-interference cancellation level. The additive white Gaussian noise power equals the self-interference power when self-interference cancellation is set to 80 dB (in the x-axis of the figure). The amount of active subcarriers (bandwidth) of the self-interference signal is varied.

interference signal and the additive white Gaussian noise. For example the legend entry 20 dB means that the total power of the self-interference signal is 20 dB above the total power of the additive white Gaussian noise. In practice, lower legend entry means better self-interference cancellation. In these results, the self-interference signal has 600 active subcarriers. In the curves, we can see that when the self-interference is suppressed to around a level of the white Gaussian noise, we get quite near to the performance level of when there is no self-interference at all. However, it seems that the self-interference still has a small effect on the detection. Even with good self-interference cancellation levels, it seems that self-interference has clear effect on the detection results. This is natural, because first of all, self-interference might have similar cyclic frequencies, but also, statistical properties of the self-interference are clearly different from those of the white Gaussian noise. The cyclostationary spectrum sensing algorithm after all is derived for the case, where the noise is pure white Gaussian noise.
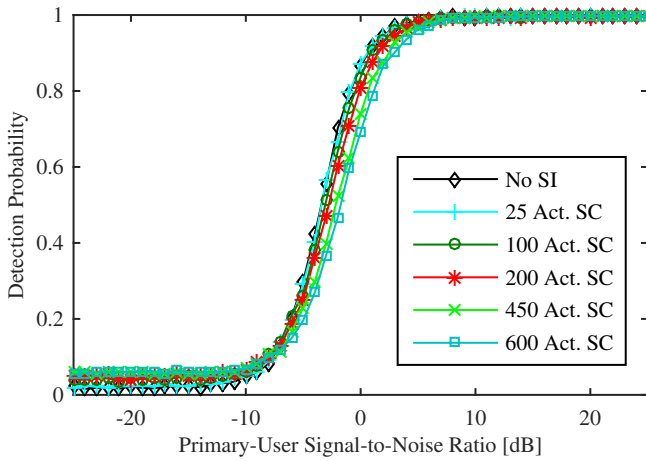
Fig. 5. Detection probability as a function of the primary-user signal-to-noise-ration when total additive white Gaussian noise power is set to the same level as the total power of the self-interference after the self-interference cancellation stages. The amount of active subcarriers (bandwidth) of the self-interference signal is varied.

Fig. 6. Detection probability as a function of the primary-user signal-to-noise-ration when total additive white Gaussian noise power is set to 5 dB lower level than the total power of the self-interference after the self-interference cancellation stages. The amount of active subcarriers (bandwidth) of the self-interference signal is varied.
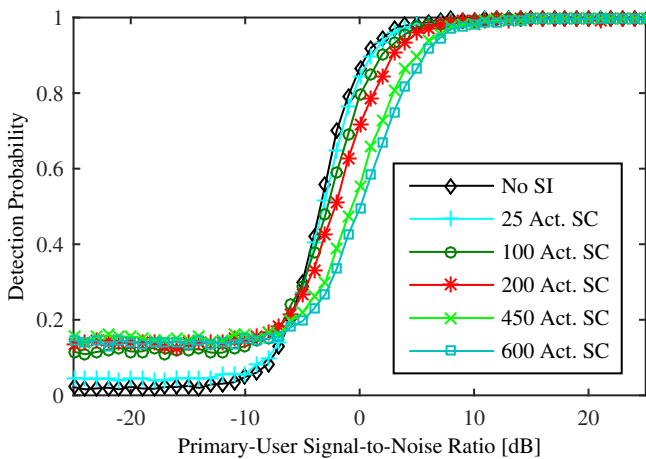
In Fig. 4, Fig. 5 and Fig. 6, the results are given for different amount of active subcarriers (denoted in the legend), which practically means different bandwidths.

In Fig. 4, the false-alarm probability is given as a function of self-interference cancellation when level of the additive white Gaussian noise is set to 80 dB below the self-interference before the self-interference cancellation. This basically means that the total self-interference power after the cancellation is at the same power level with the additive white Gaussian noise, when self-interference cancellation is 80 dB. From the figure we can see that when the power of the self-interference is very high, lower-bandwidth signal increases the false-alarm probability the most. This is because its statistical properties are less and less similar to those of the white Gaussian noise when its bandwidth is made narrower. Very high-power self-

interference is however not very interesting, because in that case the self-interference has already very huge effect on the detection performance no matter what bandwidth is used. More interesting levels of self-interference cancellation are around 80 dB or less, because there the effect of the self-interference is relatively small, and it would be attractive if the self-interference cancellation would not need to suppress the self-interference below the noise floor, and we are still able to get good detection results. We can see that by lowering the used amount of subcarriers, the false-alarm probability gets nearer and nearer to the case without the self-interference. The detection algorithm does not suffer much from the narrowband interferer. This is interesting result, because the amount of active subcarriers can be varied based on need during the primary signal detection. It should also be kept on mind, that even whilst the amount of active subcarriers is lowered, the power allocated per subcarrier increases in relation, so it is possible to get more throughput per subcarrier.

In Fig. 5 and Fig. 6, the detection probability is studied for the cases where the power of the self-interference is at the same level as and 5 dB above of, respectively, the total power of the additive white Gaussian noise. We can see that if the self-interference can be suppressed to the same level as the additive white Gaussian noise, the performance impact on the detection is relatively small, even with higher bandwidth signal. However, when the self-interference can only be suppressed 5 dB above the additive white Gaussian noise level, the self-interference has still quite clear impact on the detection result especially with higher bandwidth signals. However, the impact can be lowered by lowering the bandwidth of the secondary signal.

V. CONCLUSIONS

In this paper, the use of full-duplex radio technology was proposed for LTE unlicensed application to allow simultaneous transmission and sensing in opportunistic spectrum access. More specifically this problem was studied from the point of view of a cognitive full-duplex radio transceiver utilizing cyclostationary spectrum sensing. It was shown that the self-interference has some impact on the spectrum sensing algorithm performance if it cannot be suppressed to around the level of the noise floor of the receiver. However, if this is not possible, the impact is still relatively small even when the secondary signal is 5 dB above the noise floor. Also, the impact can be lowered by lowering the bandwidth of the secondary signal while keeping the same total transmission power.

REFERENCES

[1] Nokia Networks – White Paper, "LTE for unlicensed spectrum", 2014.

[2] Qualcomm Research – White Paper, "LTE in unlicensed spectrum: Harmonious coexistence with Wi-Fi", 2014.

[3] V. Osa, C. Herranz, J. Monserrat, and X. Gelebert, "Implementing opportunistic spectrum access in LTE-advanced," in *EURASIP Journal*

on Wireless Communications and Networking, 2012, doi: 10.1186/1687-1499-2012-99.

[4]   F. Abinader, *et al.*, "Enabling the coexistence of LTE and Wi-Fi in unlicensed bands," in *IEEE Communications Magazine*, vol. 52, no. 11, Nov. 2014.

[5]   E. Tsakalaki, O. Alrabadi, A. Tatomirescu, E. de Carvalho, and G. Pedersen, "Concurrent communication and sensing in cognitive radio devices: Challenges and enabling solution," *IEEE Trans. on Antennas and Propagation*, vol. 62, no. 3, Mar. 2014.

[6]   W. Cheng, X. Zhang, and H. Zhang, "Full duplex spectrum sensing in non-time-slotted cognitive radio networks," in *Proc. Military Communications Conference 2011*, Baltimore, MD, Nov. 2011.

[7]   T. Riihonen and R. Wichman, "Energy detection in full-duplex cognitive radios under residual self-interference," in *Proc. CROWNCOM 2014*, Oulu, Finland, Jun. 2014.

[8]   D. Bharadia, E. McMilin, and S. Katti, "Full duplex radios," in *Proc. SIGCOMM'13*, Hong Kong, August 2013.

[9]   A. Dandawate and G. Giannakis, "Statistical tests for presence of cyclostationarity," in *IEEE Trans. Signal Processing*, vol. 42, no. 9, pp. 2355-2369, 1994.

[10] V. Turunen, et al., "Implementation of cylostationary feature detector for cognitive radios," in *Proc. International Conference on Cognitive Radio Oriented Wireless Networks*, Hannover, Germany, Jun. 2009.